The 15th ISAV2025 International Conference on Acoustics and Vibration
24-25 Dec 2025 Tehran- Iran
Iranian Society of Acoustics and Vibration

Control of an Electric Actuator-Based Road Profile Simulator with Perturbation Estimation: Design and Experiment

Ahmad Sabet ghadam Alvar[a], Sadra Rafatnia[a*], Mehdi Mirzaei[a], Mohammadreza Zebardast Chavan[a]

[a] *Faculty of Mechanical Engineering, Sahand University of Technology, Tabriz, Iran.*

* *Corresponding author e-mail: sa_rafatnia@sut.ac.ir.*

Abstract

This paper presents the design and practical implementation of an observer-based feedback linearization control strategy for a scaled road profile simulator driven by an electrical actuator. To achieve high-precision tracking of the desired road profile, a feedback linearization controller is developed. Recognizing that model uncertainties and external disturbances can degrade the control performance, an extended state observer (ESO) is employed to accurately estimate these lumped perturbations. Within this framework, the system perturbation is defined as an augmented state. The ESO then utilizes measurements from a linear potentiometer transducer (LPT) to simultaneously estimate both the system state and this perturbation, enabling real-time compensation. The stability of the proposed observer is rigorously proven using Lyapunov stability theory. Comprehensive experimental results are presented, which not only demonstrate the method's excellent tracking performance and robustness but also explicitly underscore the critical role of active perturbation compensation in significantly improving the overall system's dynamic response and accuracy.

Keywords: Extended state observer; State feedback control; Observer-based controller; Road simulator system.

1. Introduction

The suspension system is a critical link between a vehicle's wheels and its chassis, serving three primary functions: improving passenger comfort by absorbing road vibrations, ensuring stability and handling by maintaining tire contact with the road, and supporting the vehicle's static and dynamic loads [1]. Specialized suspension test rigs are used to evaluate the performance and dynamics of these systems. These platforms simulate real-world driving conditions in a controlled laboratory environment, allowing engineers to precisely measure a suspension's response [2]. By using test rigs, developers can validate designs, optimize key characteristics, and accelerate research and development, all without the expense of building full-scale prototypes [3, 4].

The generation of standard road profiles is vital for evaluating vehicle suspension systems, as it provides a foundation for understanding system behavior, identifying parameters, and testing performance. Consequently, various actuators including electric motors [5], pneumatic [6], electro-mechanical [7], and hydraulic systems [8] are commonly used in the design of road profile simulators. For instance, Lin et al. [9] employed a rotating perforated disc to generate a road input consisting of two distinct bumps. Building on this, Mirzaei et al. [10] demonstrated the generation of sinusoidal road inputs with a constant amplitude and specific frequency spectrum using an electric motor. Similarly, Akbari and Lohmann [7] utilized a custom-designed actuator, while Azizi et al. [11] implemented an electro-hydraulic system for road input generation. A key limitation of these prior studies, however, is their primary focus on producing simple road profiles. Consequently, the critical challenge of designing a dedicated controller to track a desired road profile was often not addressed, a gap partly attributable to the perceived simplicity of the actuation systems themselves.

This research presents the design and practical implementation of an observer-based state feedback control for an electric actuator in a road profile simulator. The primary objective is to accurately generate road irregularities with varying amplitudes and frequencies. The simulator's mechanical structure facilitates vertical motion through four shafts and a set of guide bushings, with displacement measured by a calibrated linear potentiometer transducer (LPT) sensor. To track the desired road profiles, the proposed controller calculates the appropriate voltage for the actuator. A key feature of this approach is the use of an extended state observer (ESO) to estimate and compensate for system perturbations in real time. The effectiveness of the proposed control strategy is validated through experimental results, demonstrating superior performance compared to a standard feedback controller without an observer and highlighting the critical role of perturbation estimation. The principal innovations of this work are:

- Design and experimental validation of an observer-based feedback linearization controller for an electric-atuator road profile simulator.
- Using an ESO to estimate and compensate for system perturbations in real time and improve tracking performance.
- Practical implementation of the proposed control strategy on a test rig.

This paper is structured as follows: Following the introduction, Section 2 describes the control structure for road profile generation. Section 3 presents the mathematical model of the road simulator system. Section 4 details the design of the ESO, while Section 5 covers the controller design. Section 6 provides the experimental results and a comparative performance analysis. Finally, Section 7 concludes the paper with a summary of findings and contributions.

2. Control structure for road profile generation

The structure of the investigated control system is shown in Fig. 1. A linear potentiometer transducer (Marzak MR100) provides displacement feedback at a 100 Hz sampling rate, which is read as a voltage signal by a PCI-6052E data acquisition card. The calibrated displacement values from the DAQ are passed through a low-pass filter to reduce noise before being used by the estimator. Then the pre-filtered outputs are supplied to an extended state observer to simultaneously estimate the system states and the model's perturbations. Using the error between the reference road profile and the actual displacement, as well as the error's rate of change, the proposed controller computes a control voltage. This signal is communicated to a power supply unit via a serial interface, where it is converted, with the aid of a DC motor driver (AMD10), into a suitable operating voltage to power the electro-mechanical actuator of the road simulator system.

3. Road simulator system model

The experimental setup is detailed in Fig. 2. The road profile simulator, shown in Fig. 2(a), acts as the primary plant for the control system and is actuated to replicate various road disturbances. It forms a critical part of the complete scaled quarter-car suspension test rig, presented in Fig.

2(b). The mechanical and dynamic relationships within the test rig, including the acting forces and motion constraints, are defined in the accompanying free body diagram in Fig. 2(c).

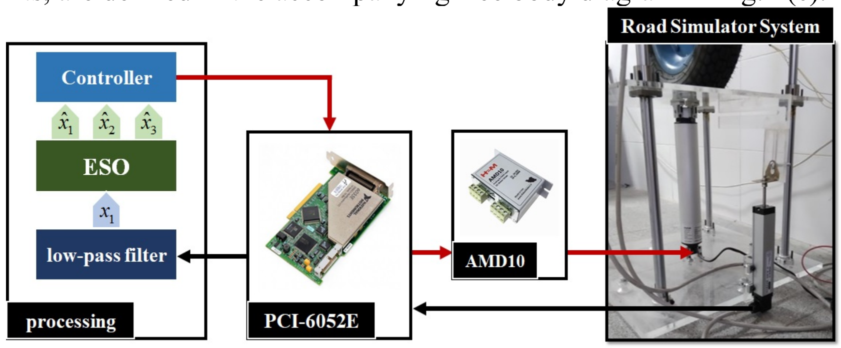

Figure 1. Proposed control structure.

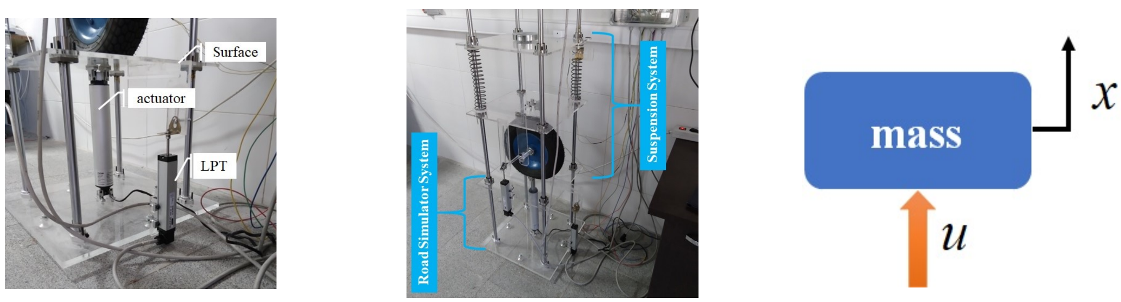

(a) (b) (c)

Figure 2. The equipment used, (a) road profile simulator, (b) scaled test rig, (c) free body diagram.

Based on Fig. 2(c) the dynamic equation for road profile simulator system can be presented as follows:

$$m\ddot{x} = u + \Delta(x, \dot{x}) \tag{1}$$

where m is the total mass on the system, u is the control force from the actuator and Δ is a bounded perturbation terms which including external disturbance, unmodeled dynamics and parametric uncertainties. By selecting the state vector as $\begin{bmatrix} x_1 & x_2 & x_3 \end{bmatrix}^T = \begin{bmatrix} x & \dot{x} & \frac{1}{m}\Delta \end{bmatrix}^T$, where x_3 is defined as an extended state, the state-space equations of the system are obtained as follows:

$$\begin{cases} \dot{x}_1 = x_2 \\ \dot{x}_2 = \dfrac{1}{m}u + x_3 \\ \dot{x}_3 = \nabla \\ y = x_1 \end{cases} \tag{2}$$

in which $\nabla = {}^{1}\!/_{m}\dot{\Delta}$ is the time derivative of the perturbation terms and is assumed to be bounded.

4. Observer design

In this research, an ESO is used to estimate the model's perturbation and provide an accurate system model. The design of the ESO is presented in this section. Based on Eq. (2), the observer's dynamic equation is as follows:

$$\begin{cases} \dot{\hat{x}}_1 = \hat{x}_2 + \beta_1\left(y - \hat{y}\right) \\ \dot{\hat{x}}_2 = \hat{x}_3 + \beta_2\left(y - \hat{y}\right) + \dfrac{1}{m}u \\ \dot{\hat{x}}_3 = \beta_3\left(y - \hat{y}\right) \\ \hat{y} = \hat{x}_1 \end{cases} \tag{3}$$

where $\beta_{i\,(i=1,2,3)}$ is the observer gains. Also, $\hat{x} = [\hat{x}_1 \quad \hat{x}_2 \quad \hat{x}_3]$ are the estimated states. By subtracting Eq. (3) from Eq. (2), the estimation error dynamics are calculated as follows:

$$\begin{cases} \dot{z}_1 = z_2 - \beta_1 z_1 \\ \dot{z}_2 = z_3 - \beta_2 z_1 \\ \dot{z}_3 = \nabla - \beta_3 z_1 \end{cases} \tag{4}$$

where $z_i = x_i - \hat{x}_i$ is the difference between the actual and estimated value of the states. According to (4), the error dynamics of the estimation errors exhibit linear behavior, and the stability of the estimation error dynamics is closely related to the proper selection of the estimator gains $\beta_{i\,(i=1,2,3)}$. The proper selection of these gains to guarantee the stability of the estimator is presented in the following theorem.

Theorem 1: If the observer gains are set as $\beta_1 = \frac{3}{\varepsilon}$, $\beta_2 = \frac{3}{\varepsilon^2}$, $\beta_3 = \frac{1}{\varepsilon^3}$, where ε is a positive free parameter, and assuming ∇ is bounded, then the estimation error dynamics will be bounded.

Proof: Defining the estimator gains as $\beta_1 = \frac{3}{\varepsilon}$, $\beta_2 = \frac{3}{\varepsilon^2}$, $\beta_3 = \frac{1}{\varepsilon^3}$ in which ε is a positive free parameter, the estimation error dynamic presented in (4) is transformed to

$$\begin{bmatrix} \dot{z}_1 \\ \dot{z}_2 \\ \dot{z}_3 \end{bmatrix} = E \begin{bmatrix} z_1 \\ z_2 \\ z_3 \end{bmatrix} + \begin{bmatrix} 0 \\ 0 \\ 1 \end{bmatrix} \nabla, \quad E = \begin{bmatrix} -\dfrac{3}{\varepsilon} & 1 & 0 \\ -\dfrac{3}{\varepsilon^2} & 0 & 1 \\ -\dfrac{1}{\varepsilon^3} & 0 & 0 \end{bmatrix} \tag{5}$$

According to bounded assumption of perturbations rate, while ∇ is bounded, the estimation error dynamic is bounded input bounded output (BIBO) if the matrix E is Hurwitz. The eigenvalues of the matrix E are found by setting the characteristic polynomial $\lambda^3 + \frac{3}{\varepsilon}\lambda^2 + \frac{3}{\varepsilon^2}\lambda + \frac{1}{\varepsilon^3}$ equals to zero, resulting three repeated eigenvalues of $\lambda = \frac{1}{\varepsilon}$. Therefore, for a suitable positive value of ε the matrix E is Hurwitz, indicating the BIBO stability of the estimation error dynamics.

5. Controller design

The control objective is to achieve exponential stability and enable precise tracking of a desired reference trajectory $x_d(t)$. The control law is synthesized in two steps. First, according to Eq. (2), a feedback linearization technique is applied to cancel the system's nonlinearities and perturbations. The equivalent control input u is formulated as:

$$u = m\left(\upsilon - \hat{x}_3\right) \tag{6}$$

here, υ is control input to be designed, and $\hat{x}_3$ is the estimate of the perturbation term ${}^{1}\!/_{m}\Delta$ provided by the ESO. Substituting (6) into the (2) effectively cancels the perturbation and yields to:

$$\dot{x}_2 = \upsilon \tag{7}$$

with the system dynamics now linearized, the second step is to design control input υ to achieve the desired closed-loop performance. With the aim of tracking a desired road profile, $x_d(t)$, the control law is defined as,

$$\upsilon = \ddot{x}_d - k_0 e - k_1 \dot{e} \tag{8}$$

in which $e(t) = x(t) - x_d(t)$ is the tracking error and $k_{i\,(i=0,1)}$ are positive gains. This control law incorporates feedforward of the reference acceleration $(\ddot{x}_d)$ and feedback of the tracking error and its derivative. By substituting (8) into (7), the resulting error dynamics for any $k_{i\,(i=0,1)} > 0$ are exponentially stable, ensuring that the tracking error $e(t)$ converges to zero.

6. Experimental results

This paper utilizes the platform illustrated in Fig. 2. for the practical implementation of the proposed controller. In this architecture, both the observer algorithm and the control input calculations are executed on a workstation equipped with an Intel® Core™ i9-12900K processor (3.2 GHz base frequency, 30 MB cache). Sensor data is transmitted via a serial port to Simulink software, where the control voltage is computed. This voltage is then sent to a 24V DC motor driver, which subsequently applies it to the electrical actuator, thereby completing the hardware-in-the-loop (HIL) implementation.

In the section the result of the proposed controller for different road profiles shown in Table 1 is presented. In the first result, the efficiency of the proposed observer in estimation of the states and perturbation is presented in Fig. 3, for different values of free parameter ε. According to Fig. 3, the estimation error is reduced by decreasing the value of ε. Also as depicted in Fig. 3(d), the root mean square (RMS) of estimation errors are reduced by decreasing the free parameter up to an acceptable range. This result was previously proven in Theorem 1. However, reducing the parameter beyond a certain point also amplifies measurement noise, which causes an increase in the estimation error. Therefore, the value of $\varepsilon = 0.01$ is selected a reasonable value for the free parameter of the observer.

After confirming the efficiency of the proposed observer, the tracking performance of the controller for a harmonic road profile is shown in Fig. 4. Since all the results are obtained from real-time experiments, the measured signals naturally contain sensor noise. To further demonstrate the benefit of the estimation algorithm, the proposed method is compared with a controller that does not use the perturbation term. In this comparative case, where the observer is omitted, the controller reduces to the standard feedback control method. Note that, these results are achieved by selecting control gains as $k_0 = 120$ and $k_1 = 120$. Based on Fig. 4 and the root mean squere of tracking error presented in Fig. 4(d), the proposed observer-based controller demonstrates significantly superior performance, reducing the RMS tracking error. This consistent improvement confirms the critical role of the observer in enhancing tracking accuracy by estimating and canceling system perturbations.

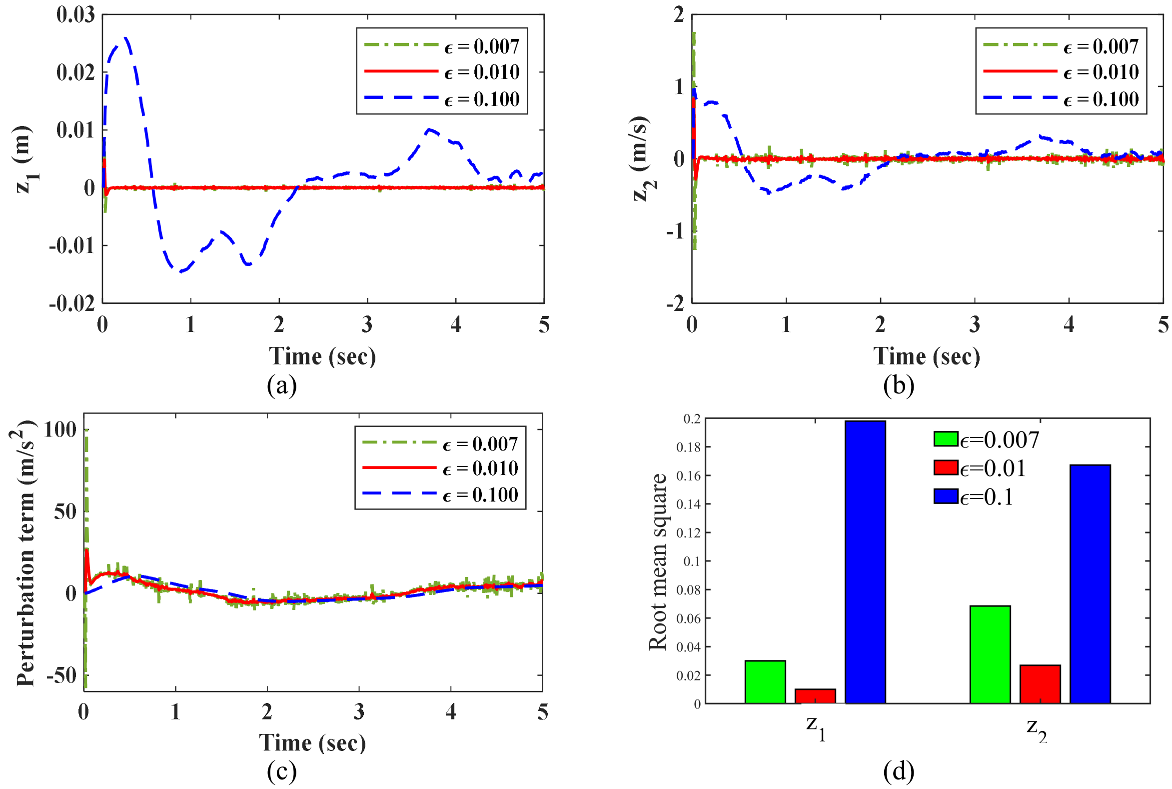

Figure 3. Estimation error in Test 1, (a) displacement, (b) velocity, (c) perturbations, (d) Root mean square.

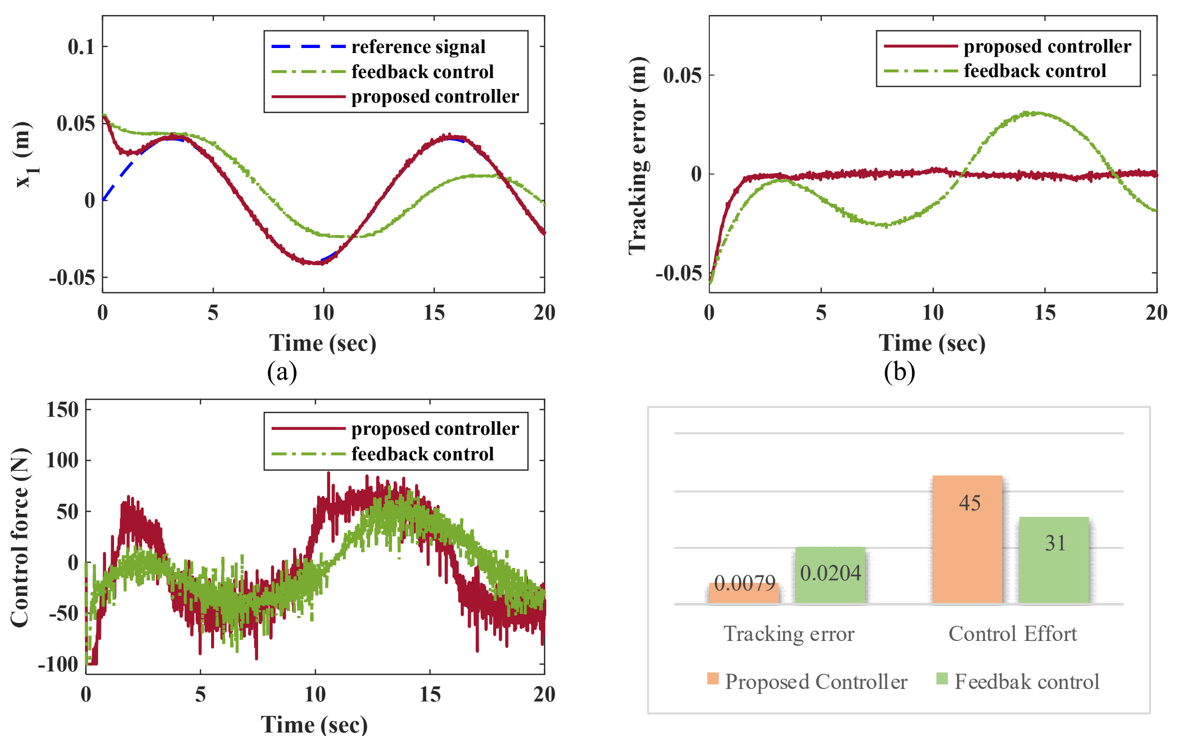

Figure 4. Control result in Test 1, (a) Tracking the desired road profile, (b) Tracking error, (c) Control force, (d) Root mean square of tracking error and control effort.

Table 1. Road profile reference signal equations.

Tests	Desired road profile equations
Test 1	$x_r = 0.04\sin(0.5t)$
Test 2	$x_r = -0.01(0.2 - \sin(0.3\pi t)) - 0.005\sin(0.5\pi t)$
Test 3	$x_r = 0.01\sin(2t)$

To demonstrate the independence of the proposed control method from the desired road profile, the results for two additional profiles are presented in Figs. 5 and 6. The results show that the proposed controller, which incorporates the observer, generates a more aggressive and proactive control signal that actively cancels out perturbations. This capability allows the system to respond more quickly and accurately to the reference signal, leading to superior tracking performance. In contrast, the standard feedback controller, lacking perturbation estimation, produces undesirable results because it can only react to the tracking error after it has occurred, without the ability to preemptively compensate for the system's internal dynamics and disturbances. Moreover, Fig. 5 also demonstrates that the proposed controller achieves better tracking performance while using less control effort compared to the simple feedback controller.

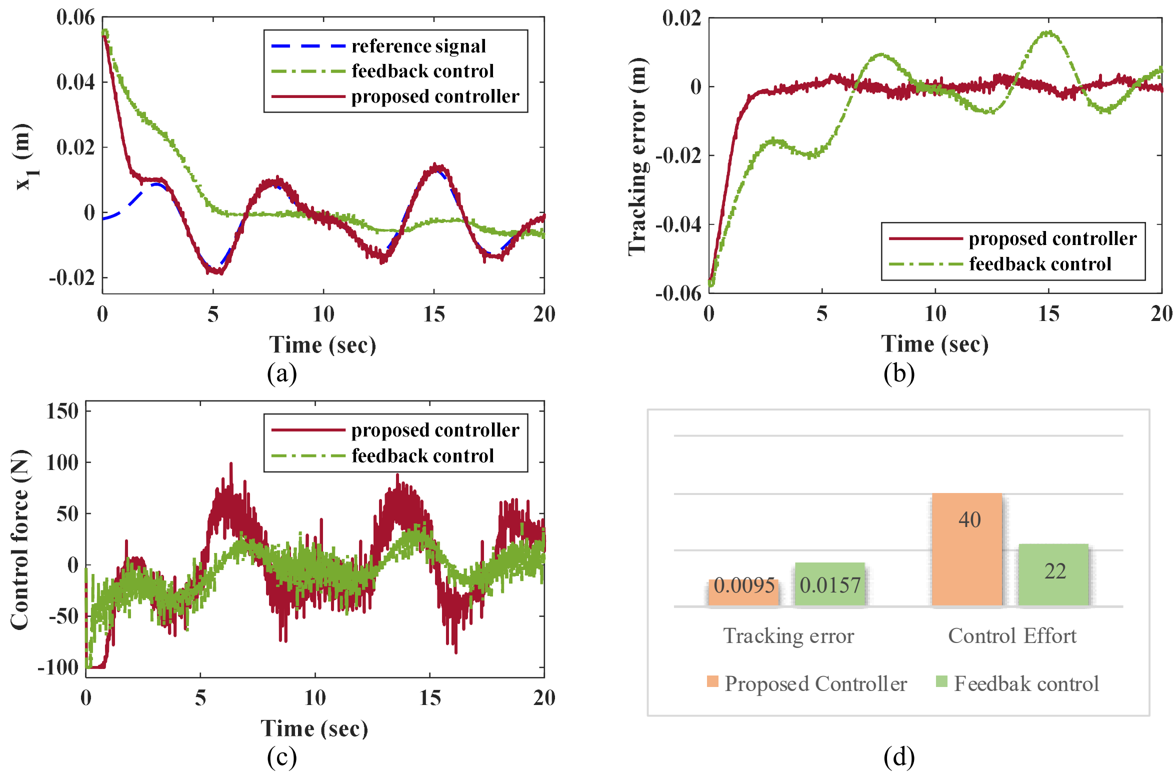

Figure 5. Control result in Test 2, (a) Tracking the desired road profile, (b) Tracking error, (c) Control force, (d) Root mean square of tracking error and control effort.

7. Conclusion

This research designed and experimentally validated an observer-based state feedback linearization controller for a road profile simulator. By integrating an ESO, the observer effectively estimated and compensated for system perturbations and unmeasurable states in real-time. Experimental results demonstrated the controller's superior tracking performance across various road profiles, significantly outperforming a standard feedback controller that lacked perturbation estimation. The ESO's critical role enabled a more proactive and robust control action, directly translating to a substantial reduction in tracking error. This study conclusively establishes the ESO-based approach as a highly effective method for achieving accurate road profile simulation.

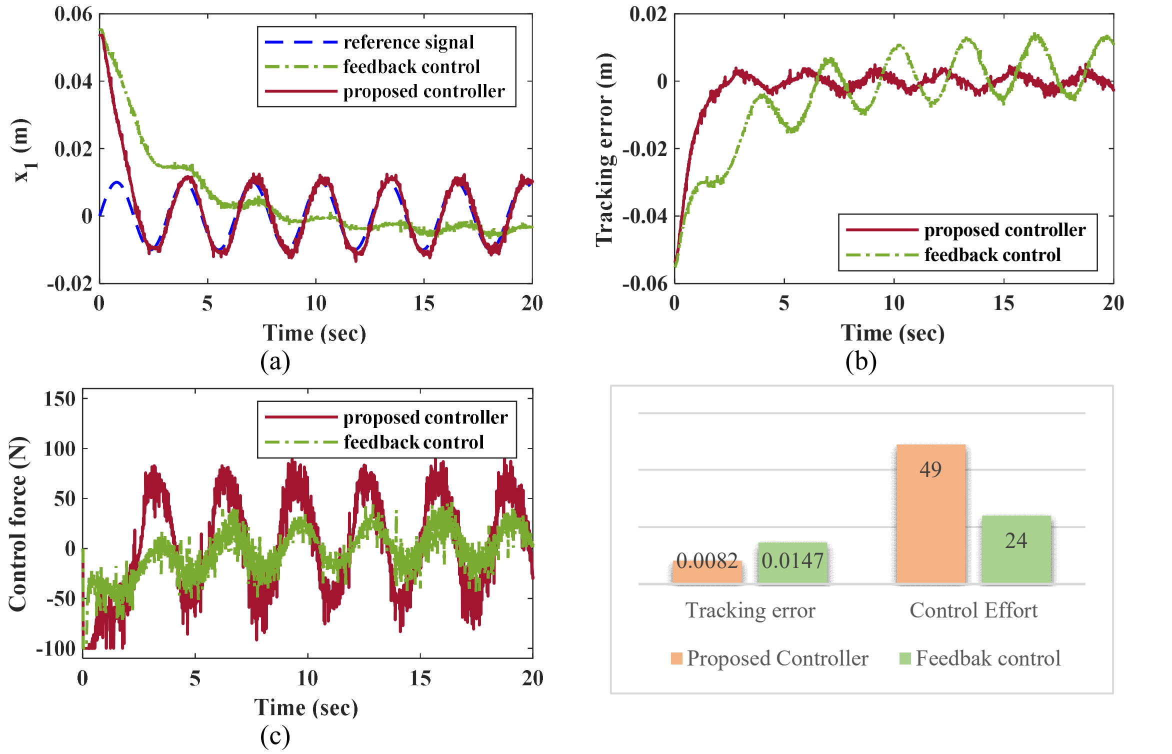

Figure 6. Control result in Test 3, (a) Tracking the desired road profile, (b) Tracking error, (c) Control force, (d) Root mean square of tracking error and control effort.

REFERENCES

1. Aghasizade, S., Mirzaei, M., & Rafatnia, S. "Novel constrained control of active suspension system integrated with anti-lock braking system based on 14-degree of freedom vehicle model", *Proceedings of the Institution of Mechanical Engineers, Part K: Journal of Multi-body Dynamics* **232** (4), 501-520 (2018).
2. Sisi, Z. A., Mirzaei, M., & Rafatnia, S. "Estimation of vehicle suspension dynamics with data fusion for correcting measurement errors", *Measurement* **231**, 114438 (2024).
3. Ahangari Sisi, Z., Mirzaei, M., & Rafatnia, S. "New strategy to perturbation estimation and constrained control of vehicle suspension system", *Proceedings of the Institution of Mechanical Engineers, Part D: Journal of Automobile Engineering* **09544070251324262** (2024).
4. Ahangari Sisi, Z., Mirzaei, M., & Rafatnia, S. "Input-Saturated Control of Active Suspension System Using Fuzzy-Scheduled Estimation of Model Uncertainties and Road Disturbances", *International Journal of Robust and Nonlinear Control*. https://doi.org/10.1002/rnc.70180 (2025).
5. S. Ka'ka, S. Himran, "Pneumatic actuator as vertical dynamic load simulator on the suspension mechanism of a quarter vehicle wheels", *ARPN Journal of Engineering and Applied Sciences* **12**, 6975-6980 (2017).
6. G. Koch, E. Pellegrini, "Design and modeling of a quarter-vehicle test rig for active suspension control", Lehrstuhl für Regelungstechnik, (2010).
7. A. Akbari, B. Lohmann, "Output feedback H∞/GH 2 preview control of active vehicle suspensions: a comparison study of LQG preview", *Journal of Vehicle System Dynamics* **48**, 1475-1494 (2010).
8. D. Chindamo, M. Gadola, "Design of a road simulator for motorcycle applications", *Journal of Applied Sciences* **7**, 1220 (2017).
9. J. Lin, K. W. E. Cheng, "Adaptive sliding mode technique-based electromagnetic suspension system with linear switched reluctance actuator", *Journal of IET Electric Power Applications* **9**, 50-59 (2015).
10. M. M. Salmani Arani, M. Mirzaei, "Identification of a nonlinear model for elements of a test rig of quarter car suspension system", *Journal of Modares Mechanical Engineering* **15,** 136-142 (2016).
11. M. J. Azizi, M. Mirzaei, S. Rafatnia, T. F. Nodeh, "Design and experimental evaluation of road excitation simulator actuated by electro-hydraulic system", *Journal of Theoretical and Applied Vibration and Acoustics* **10,** 34-49 (2025).